JACS
JOURNAL OF THE AMERICAN CHEMICAL SOCIETY
Article
pubs.acs.org/JACS

The Mechanism of Hydroaminoalkylation Catalyzed by Group 5 Metal Binaphtholate Complexes

Alexander L. Reznichenko and Kai C. Hultzsch*

Department of Chemistry and Chemical Biology, Rutgers, The State University of New Jersey, 610 Taylor Road, Piscataway, New Jersey 08854-8087, United States

Supporting Information

ABSTRACT: The intermolecular hydroaminoalkylation of unactivated alkenes and vinyl arenes with secondary amines occurs readily in the presence of tantalum and niobium binaphtholate catalysts with high regio- and enantioselectivity (up to 98% ee). Mechanistic studies have been conducted in order to determine the kinetic order of the reaction in all reagents and elucidate the rate- and stereodetermining steps. The effects of substrate steric and electronic properties on the overall reaction rate have been evaluated. The reaction is first order in amine and the catalyst, while exhibiting saturation in alkene at high alkene concentration. Unproductive reaction events including reversible amine binding and arene C−H activation have been observed. The formation of the metallaaziridine is a fast reversible nondissociative process and the overall reaction rate is limited either by amide exchange or alkene insertion, as supported by reaction kinetics, kinetic isotope effects, and isotopic labeling studies. These results suggest that the catalytic activity can be enhanced by employing a more electron-deficient ligand backbone.

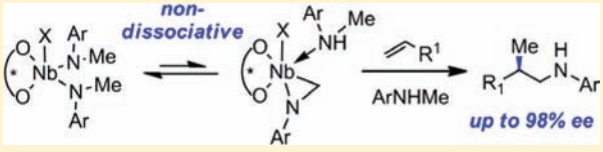

INTRODUCTION

The catalytic inter- and intramolecular hydroaminoalkylation is an atom-economical process for the synthesis of industrial and pharmaceutical valuable amines in which an α-amino C−H moiety is added across an unsaturated carbon−carbon bond (Scheme 1).[1−3] While initial reports on catalytic hydroaminoalkylation surfaced more than 30 years ago,[4] this reaction has become a subject of intensive research efforts only recently.[1,5−8] Although few examples of main group metal-catalyzed α-C−H addition of amines to alkenes are known,[9] a majority of hydroaminoalkylation catalysts are based on d^0 group 4 and group 5 metal complexes (Chart 1).

Scheme 1. Inter- and Intramolecular Hydroaminoalkylation

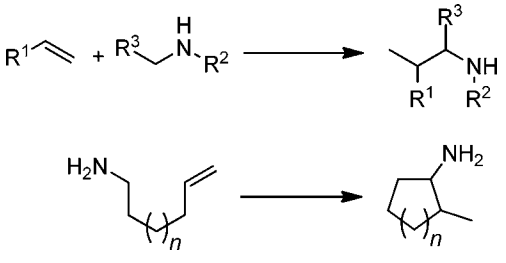

In line with earlier observations,[4] Herzon and Hartwig have demonstrated that the homoleptic tantalum amide **I**[5a] and the heteroleptic chloro bisamide **II**[5b] are active catalysts for the intermolecular hydroaminoalkylation of unactivated olefins with secondary amines, with the latter catalyst being more reactive and applicable to a broader range of substrates, including dialkylamines.

Chart 1. Selected Group 4 and Group 5 Metal Hydroaminoalkylation Catalysts

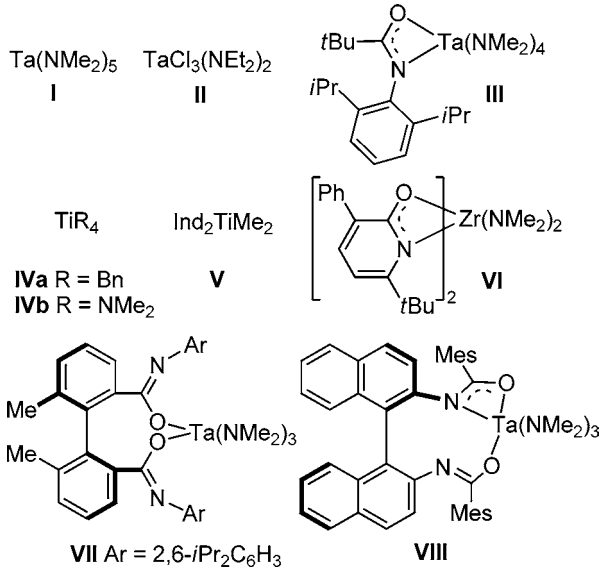

More recently, Schafer and co-workers have developed a family of various amidate tantalum catalysts, such as **III** and similar structures.[5c] The observation of hydroaminoalkylation as a side reaction of hydroamination[6a] has sparked the development of group 4 metal hydroaminoalkylation catalysts. The homoleptic tetrabenzyl titanium **IVa**[6b,c] or bis(indenyl)

Received: December 22, 2011
Published: January 19, 2012

   dx.doi.org/10.1021/ja211945m | J. Am. Chem. Soc. 2012, 134, 3300−3311

complex **V**[6e] was shown to catalyze intra- and intermolecular hydroaminoalkylations with notable reactivity for *primary* alkenyl amines in the intramolecular process. Catalysts for asymmetric intermolecular hydroaminoalkylation have been developed employing κ^1-[5c] and κ^1-/κ^2-amidate[5d,e] frameworks. In line with the selectivity trends previously reported for the asymmetric hydroamination with related zirconium amidate complexes,[10] the sterically more hindered chelating κ^2-amidates **VIII** displayed higher enantioselectivities (up to 93% ee for selected substrates).[5d,e] However, in contrast to the reactivity trends observed in intramolecular hydroaminations, the sterically and electronically more saturated complex **VIII** was reported to be more active than the sterically more accessible and electronically unsaturated complex **VII**.

The general mechanism of catalytic hydroaminoalkylation was proposed in the early studies dealing with group 5 metal catalysts (Scheme 2).[4b] The key step of the catalytic cycle is

Scheme 2. Mechanism of Intermolecular Hydroaminoalkylation

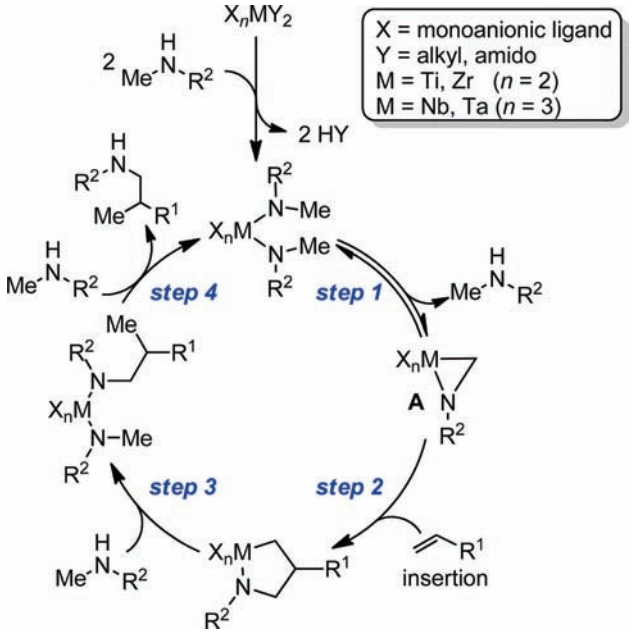

believed to be the C−H activation of the bisamide leading to the metallaaziridine **A** (Scheme 2, step 1). Subsequent alkene insertion (Scheme 2, step 2), protonolysis of the metal−carbon bond (Scheme 2, step 3), and amide exchange (Scheme 2, step 4) completes the catalytic cycle. The insertive reactivity of metallaaziridines has already been used in other synthetic applications.[11] Only few mechanistic details on the reversibility and relative feasibility of steps 1−4 are available. Herzon and Hartwig have demonstrated that the formation of the metallaaziridine **A** is reversible in the reaction catalyzed by **I**,[5a] whereas step 1 is virtually irreversible in the case of catalyst **II**,[5b] as suggested by isotopic labeling studies. The same studies implicate that steps 2 and 3 should be fast, as the catalyst has no metal−carbon bond in its resting state. Recently, Doye and coworkers reported that the intramolecular hydroaminoalkylation of primary aminoalkenes catalyzed by $Ti(NMe_2)_4$ (**IVb**) involves a rate-limiting C−H activation step, as indicated by a pronounced kinetic isotope effect.[6f] The lack of a sterically demanding spectator ligand in **IVb** resulted in catalyst aggregation and a complex kinetic behavior at higher catalyst concentrations.[6f]

Recently, we have communicated[8] that 3,3′-silyl-substituted binaphtholate niobium and tantalum complexes[12] (Chart 2) are

Chart 2. 3,3′-Silyl-Substituted Binaphtholate Niobium and Tantalum Catalysts for Asymmetric Intermolecular Hydroaminoalkylation

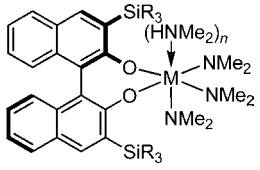

M = Ta, Nb

	SiR_3	*n*
1a-M	$SiiPr_2Me$	1 (Ta) / 0 (Nb)
1b-M	$SiPh_2Me$	1
1c-M	$SiMe_2tBu$	0
1d-M	$SiMe_3$	1

efficient catalysts for the intermolecular hydroaminoalkylation. The lack of more detailed mechanistic and kinetic information prompted us to study the mechanism of this transformation in greater depth. Herein we present the results from our investigations into the scope and limitations of catalysts **1-M** (M = Nb, Ta) in the hydroaminoalkylation reaction and a detailed analysis of the reaction mechanism.

RESULTS AND DISCUSSION

Initial Catalyst Screening. The reaction of 1-octene with *N*-methylaniline was chosen as a model reaction to evaluate the different tantalum and niobium catalysts (Table 1). Complexes **1a−d** showed good activity at 150 °C to form the branched hydroaminoalkylation products exclusively. The rate of the reaction generally increases with decreasing steric demand of the silyl substituent of the binaphtholate ligand. The sterically least demanding trimethylsilyl-substituted complexes **1d-Ta** and **1d-Nb** displayed the highest activity, but also the lowest selectivity in this series. Sterically more encumbered catalysts with triphenylsilyl and benzyldiphenylsilyl substituents produced only traces of product even at 170 °C.[8] Under our standard conditions at 150 °C, the methyldiphenylsilyl-substituted complexes **1b-Nb** and **1b-Ta** exhibited the highest selectivity (Table 1, entries 3 and 5), whereas the slightly more demanding methyldiisopropylsilyl-substituted complexes **1a-Nb** and **1a-Ta** displayed slightly lower selectivities than **1b**. The niobium complexes were generally more active than their tantalum analogues, but the enantioselectivities were quite comparable in most cases. The discrepancy of reactivity of the tantalum and niobium complexes is even more pronounced at lower temperatures, as the tantalum complexes gave poor reactivity below 140 °C, while the niobium catalyst **1b-Nb** was reactive even at 100 °C to give the highest selectivity of 81% ee for this model reaction (Table 1, entry 7). Notably, **1b-Nb** appears to be more active at 100 °C than the chiral catalyst **VII** at 130 °C.[5c] The relative reactivity of tantalum and niobium complexes depends on the catalyst structure; while in some instances niobium was found to be superior to tantalum,[4b] niobium was claimed to be inactive in other.[5d,e]

The most reactive catalyst **1b-Nb** was then used to evaluate the scope of the reaction at 140 °C (optimal reaction time) and 100 °C (optimal enantioselectivity).

dx.doi.org/10.1021/ja211945m | J. Am. Chem. Soc. 2012, 134, 3300−3311

Table 1. Catalytic Asymmetric Hydroaminoalkylation of 1-Octene with *N*-Methylaniline using Binaphtholate Tantalum and Niobium Complexes[a]

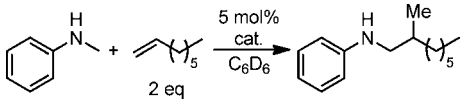

entry	cat.	*T*, °C; *t*, h	yield, %[b]	ee, %[c]
1	**1a-Ta**	150; 31	89	65
2	**1a-Nb**	150; 20	93	60
3	**1b-Ta**	150; 14	88	72
4	**1b-Ta**	130; 65	89	73
5	**1b-Nb**	150; 7	85	72
6	**1b-Nb**	130; 58	91	79
7	**1b-Nb**	100; 105	92	81
8	**1c-Ta**	150; 12	79	49
9	**1c-Nb**	150; 8	72	61
10	**1d-Ta**	150; 5	87	34
11	**1d-Nb**	150; 3	91	54

[a]Conditions: *N*-methylaniline (0.2 mmol), 1-octene (0.4 mmol), cat. (0.01 mmol, 5 mol %), C_6D_6 (0.25 mL), Ar atm. [b]Isolated yield of the corresponding *N*-benzamide. [c]Determined by chiral HPLC of the *N*-benzamide.

Scope in Amine. As shown in Table 2, various *N*-methylanilines bearing both electron-withdrawing and electron-donating substituents exhibit similar reactivities and selectivities in reactions involving terminal olefins. The niobium complex **1b-Nb** displayed systematically higher reactivity in comparison to its tantalum analogue **1b-Ta**. The unsymmetric dialkylamine *N*-benzylmethylamine (Scheme 3) was less reactive than arylalkylamines. Here, the difference in reactivity of niobium and tantalum was even more pronounced, with the niobium complex reacting at 150 °C, while tantalum required a significantly higher reaction temperature of 180 °C. The reactions of *N*-methylaniline derivatives provide enantioselectivities in a relatively narrow range of 66−80% ee at 140 °C, while the reaction of *N*-benzylmethylamine was significantly less selective. None of the reactions produced any detectable amount of the linear addition product; however, the reaction of *N*-benzylmethylamine produced the regioisomer **11b** originating from activation of the benzylic position as a minor byproduct (Scheme 3). The regioselective formation of **11a** is in agreement with observations for **II**,[5b] but is in remarkable contrast to selectivities found for the amidate **III**.[5c]

The sluggish reactivity of a secondary alkylamino group is further manifested by the absence of product formation in the reaction of 1-octene with *N*-ethylaniline, pyrrolidine, and tetrahydroisoquinoline at 150−180 °C. It should be noted that these and similar amines lacking an *N*-methyl group were reactive with tantalum amidate catalyst **III**[5c] and Ind_2TiMe_2 (**V**).[6e] While multiple mechanistic scenarios may account for the enhanced regioselectivity of catalysts **1b-Ta** and **1b-Nb**, it is notable that their preference of activating the *N*-methyl group is greater than that of other known group 4 and group 5 metal catalysts.

Scope in Alkene. Linear, α- and β-branched terminal olefins exhibit comparable reactivities in hydroaminoalkylations (Table 2, entries 1−20), which seems to be remarkable in comparison to a significant diminished reactivity of α-branched terminal olefins observed in the intermolecular hydroamination.[13] Higher enantioselectivities were observed for sterically more demanding alkenes (Table 2, entries 2, 3, 11, and 16) as well at lower reaction temperatures (Table 2, entries 4, 6, 10, 12, and 17). Unactivated 1,2-disubstituted alkenes, such as cyclohexene, were unreactive; however, the more activated norbornene provided the corresponding product **8**, though only in moderate yield due to formation of poly(norbornene) as a side reaction. Methylene cyclohexane exhibited lower reactivity because of the *gem*-disubstituted double bond. Other 1,1-disubstituted alkenes, such as α-methylstyrene, were unreactive. Notably, all reactions proceeded with excellent branched to linear regioselectivity exceeding 50:1. This also includes the reaction of **2d** with styrene at 100 °C, which produced the branched product (*S*)-(−)-**10**[14] with >30:1 regioselectivity in 71% ee when using (*R*)-**1**-Nb (Table 2, entry 21). The highest enantioselectivity of 98% ee was observed in the reaction of *N*-methylaniline (**2a**) with trimethyl(vinyl)silane at 100 °C (Table 2, entry 17).

Isotopic labeling studies have been used previously in intermolecular (**I**[5a] and **II**[5b]) and intramolecular (**IVb**[6f]) hydroaminoalkylations. We have attempted to use this approach in order to gain further insight into the mechanism of the reaction catalyzed by **1**. Reaction of *N*-(methyl-d_3)-aniline with vinylcyclohexane catalyzed by **1b-Ta** led to a product with significantly depleted deuterium content at the methylene group and significant deuterium incorporation into the *ortho*-positions of the aryl ring (Scheme 4). This leakage of deuterium from the methylene group was interpreted as an indicator of a reversible metallaaziridine formation (Scheme 2, step 1),[5a,b] whereas the incorporation of deuterium into the aryl ring should result from the intramolecular C−H activation via cyclometalation (Scheme 4).[5a]

An important feature is the low incorporation of deuterium into the methyl group compared to that of the *ortho*-position of the aryl ring. Although 1.67 equiv deuterium is released from the original CD_3 group, only 33% of the methyl groups in the product are labeled (= 11% total deuteration of CH_3), suggesting that the protonation (Scheme 2, step 3) proceeds predominantly with an N-proteo amine rather than an N-deutero amine, which is in agreement with observations for **I**[5a] and **IVb**.[6f] The reaction of *N*-(methyl-d_3)-aniline with a catalytic amount of **1b-Ta** (1 mol %) in the absence of alkene resulted in a similar incorporation of deuterium into the *ortho*-position of the aniline (42% deuterium after 2 h at 150 °C), indicating that the reversible cyclometalation is likely preceding

dx.doi.org/10.1021/ja211945m | *J. Am. Chem. Soc.* 2012, 134, 3300−3311

Table 2. Substrate Scope in the Intermolecular Asymmetric Hydroaminoalkylation Catalyzed by 1b-M (M = Ta, Nb)[a]

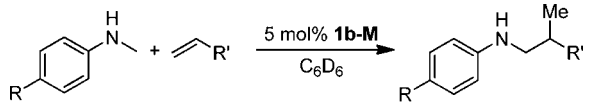

2a R = H
2b R = F
2c R = Cl
2d R = OMe

Entry	Amine	Alkene	Product	M	T, °C	t, h	Yield, %	ee, %[b]
1	2a	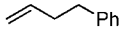	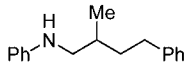 **3**	Ta	140	24	79	67
2	2a			Nb	140	12	71	70
3	2a		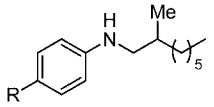 **4a–d**	Nb	140	7	85	73
4	2a			Nb	100	105	92	81
5	2b			Nb	140	7	95	66
6	2b			Nb	100	69	89	82
7	2c			Nb	140	6	90	67
8	2d			Nb	140	5	89	74
9	2d	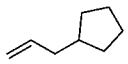	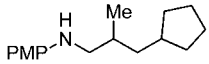 **5**	Nb	140	13	88	71
10	2d			Nb	100	38	89	81
11	2a		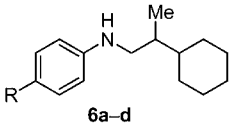 **6a–d**	Nb	140	9	89	80
12	2a			Nb	100	60	92	91
13	2b			Nb	140	8	93	73[c]
14	2c			Nb	140	8	82	71[d]
15	2d			Nb	140	5	87	75[d]
16	2a	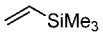	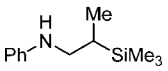 **7**	Nb	140	9	93	92
17	2a			Nb	100	48	82	98
18	2a		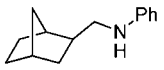 **8**	Ta	140	40	65	61
19	2a			Nb	140	12	61	59
20	2a		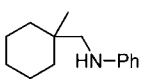 **9**	Nb	140	48	72	--
21	2d	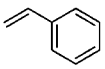	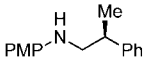 **10**	Nb	100	48	73	71[d]

[a]Reaction conditions: amine (0.2 mmol), alkene (0.4 mmol), **1b-M** (0.01 mmol, 5 mol %), C_6D_6, Ar atm. [b]Determined by chiral HPLC of the corresponding *N*-benzamide. [c]Determined by ^{1}H NMR spectroscopy of (*S*)-Mosher amide. [d]Determined by chiral HPLC.

Scheme 3. Hydroaminoalkylation of *N*-Benzylmethylamine

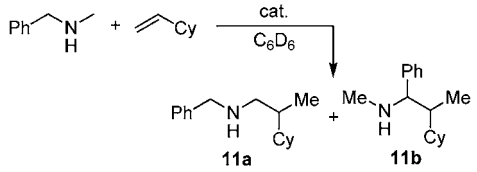

11a **11b**

cat.	T, °C	t, h	11a:11b	Yield 11a, %	ee 11a, %
10 mol% **1b-Ta**	180	52	10:1	59	35
7 mol% **1b-Nb**	150	48	8:1	63	25

the insertion (Scheme 2, step 2) and is not necessarily part of the catalytic cycle.

A strikingly different outcome was observed when **1b-Nb** was used instead of **1b-Ta**. In this case, the reaction of *N*-(methyl-d_3)-aniline with vinylcyclohexane proceeded with almost complete retention of deuterium in the methylene group and no *ortho*-metalation of the aniline aromatic ring was observed (Scheme 5). Thus, it seems that the lower reactivity of tantalum compared to niobium can be attributed in part to the formation of a cyclometalated species that removes the catalyst from its active state.

The absence of *ortho*-metalation for the niobium catalyst supports the hypothesis that this process is nonproductive in character. The retention of deuterium in the methylene group is similar to that observed with **II**,[5b] which was interpreted as a result of irreversible C–H activation (Scheme 2, step 1) followed by rapid olefin insertion (Scheme 2, step 2). However, one feature of the reaction catalyzed by **1b-Nb** is unprecedented, which is almost complete (96%) deuteration of the methyl group of the product, while the reaction with catalyst **II** resulted in only 30% deuteration in our hands. Even more strikingly, when the reaction was stopped at ~20% conversion and starting material and product were recovered, high deuterium incorporation into the methyl group of the product (91%) along with almost complete retention of

dx.doi.org/10.1021/ja211945m | J. Am. Chem. Soc. 2012, 134, 3300–3311

Scheme 4

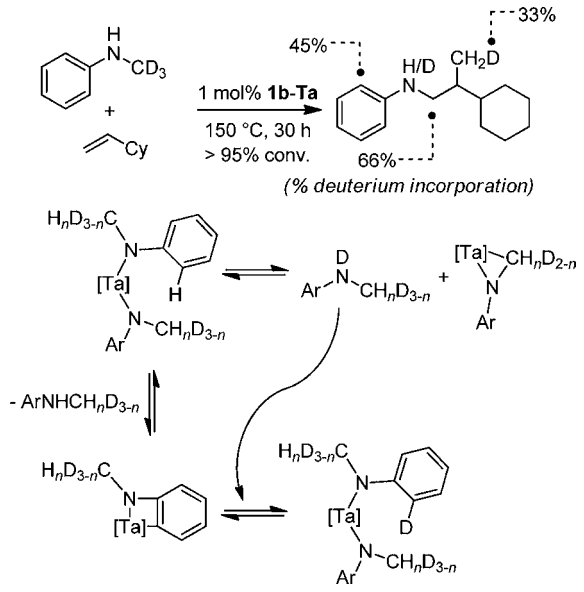

Scheme 5

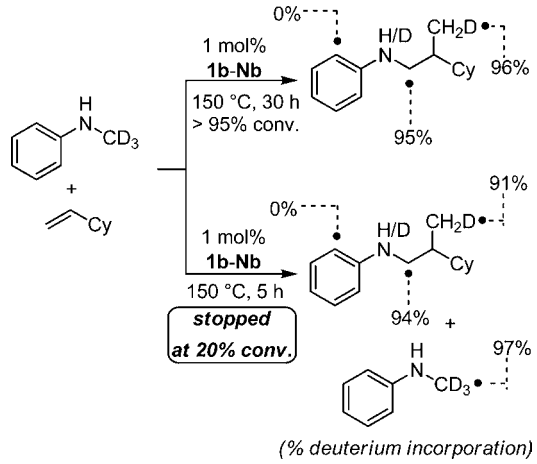

deuterium in the starting material (97%) was observed (Scheme 5). Unfortunately, direct quantitative determination of the extend of deuteration of the amine NH group is complicated due to broad and overlapping signals in the reaction mixture and loss of the amine deuterium during workup. However, complete retention of deuterium in the molecule of the starting material suggests that most of the N–H groups are still undeuterated at low conversion. The high degree of monodeuteration of the methyl group in the product indicates that protonolysis of the azametallacyclopentane intermediate (Scheme 2, step 3) occurs almost exclusively with an N-deutero amine. Thus, the deuterium from the *N*-(methyl-d_3)-aniline starting material is transferred with high selectivity to the methyl group in the product. Although direct catalytic protonolysis of the metal–alkyl bond with another C–H bond via σ-bond metathesis is known,[15] we propose a more realistic mechanistic scenario involving the nondissociative formation of the metallaaziridine **A*PhNHMe** (Scheme 6, step 1), which retains the coordinated amine molecule during the insertion (Scheme 6, step 2). The subsequent protonolysis (Scheme 6, step 3) proceeds in an intramolecular fashion without participation of an external amine.

Several important consequences arise from the mechanism depicted in Scheme 6. First, the lack of deuterium scrambling from the methylene position cannot serve as a proof[5b] of an irreversible character of step 1. In fact, since a nondissociative metallaaziridine formation can be reversed in a fully degenerate process, reversible metallaaziridine formation will still result in retention of deuterium. Indeed, prolonged heating of **1b-M** (M = Ta, Nb) in the presence or absence of a slight excess of **2a** (0–10 equiv) to 100–130 °C did not result in conversion to, or even observation of, the metallaaziridine **A*PhNHMe** according to ^{1}H NMR spectroscopy. However, the catalytic reactions proceeded smoothly in the presence of an alkene, which is another indicator that step 1 is reversible and the equilibrium is shifted toward the bisamide species. Second, the presence of a coordinated amine during the insertion step 2 can result in a concerted protonolysis-assisted insertion, so that steps 2 and 3 could merge into a single, concerted reaction step. This process would be reminiscent to a number of early transition metal hydroamination catalysts that have been proposed to operate via a protonolysis-assisted alkene insertion into a metal–nitrogen bond.[16] Quenching of a reaction mixture containing 25 mol % **1b-M** (M = Ta, Nb) at ca. 40% conversion with 12 M DCl/D$_2$O did not result in any noticeable deuterium incorporation into the methyl group of either product **6a** or starting material **2a**, further suggesting that the concentration of metallaaziridine and metal–alkyl species remains low over the course of the reaction.

The incomplete (<98%) deuteration of the product methyl group (Scheme 5) could arise from intermolecular protonation of the metal–carbon bond by an external amine. However, no measurable deuterium incorporation was observed in the reaction of *N*-deutero-*N*-methyl-aniline with vinylcyclohexane using 1 mol % **1b-Nb** (Scheme 7). On the other hand, the same reaction with *N*-(methyl-d_3)-aniline using 7 mol % **1b-Nb** led to a diminished deuteration of the methyl group (71%) and depletion of deuterium from the methylene group (85%). These observations suggest that the residual protonation results

Scheme 6. Nondissociative Metallaaziridine Formation and Intramolecular Proton Delivery

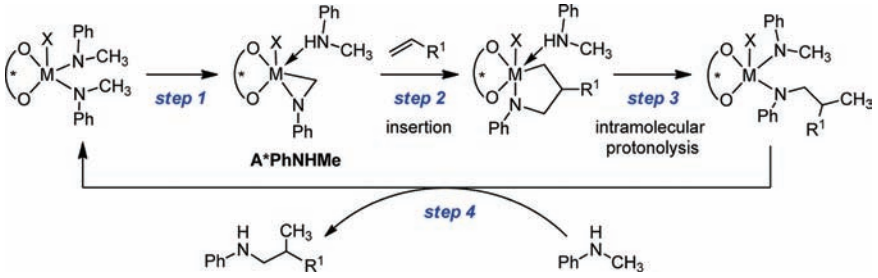

dx.doi.org/10.1021/ja211945m | J. Am. Chem. Soc. 2012, 134, 3300–3311

Scheme 7

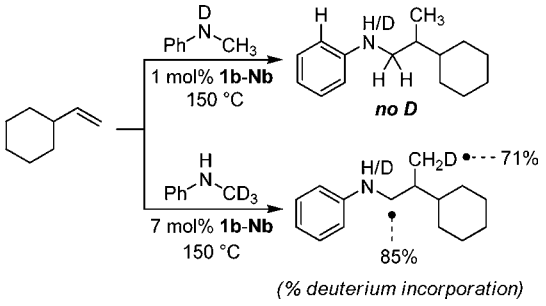

from C−H activation of the dimethylamido groups of the precatalyst rather than from outer-sphere protonolysis.

As mentioned previously, a notable feature of catalysts **1** is a pronounced preference for activation of primary over secondary C−H bonds resulting in a lack of reactivity toward substrates without an N-methyl group. Previously, an isotopic labeling study with **II** suggested that hampered C−H activation limited the hydroaminoalkylation of secondary C−H bonds.[5b] In our case, although no hydroaminoalkylation product was formed with *N*-ethyl-aniline using either **1b-Ta** or **1b-Nb**, *N*-(ethyl-d_5)-aniline displayed some deuterium scrambling after 50 h at 150 °C in the presence of **1b-Ta** (Scheme 8).

Scheme 8

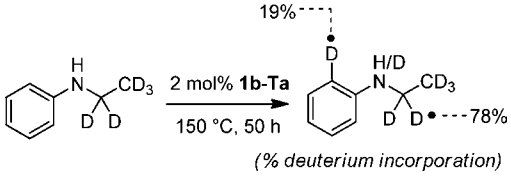

Despite the rate of deuterium exchange being considerably slower than in case of *N*-(methyl-d_3)-aniline, it seems that C−H activation of a secondary C−H bond is not prohibited. The lack of reactivity of secondary C−H bonds should therefore result from hampered alkene insertion (step 2) rather than hampered C−H activation (step 1).

The stereochemistry of olefin insertion into a metal−ligand bond can provide invaluable information on the details of the reaction mechanism. For example, the stereochemistry of the inter-[17] and intramolecular[18] olefin insertion into a palladium−amide bond, as well as the intramolecular gold-[19] and Brønsted acid-catalyzed[20] cyclization of alkenyl sulfonamides, has been investigated in the context of the hydroamination reaction.

We have performed the reaction of norbornene with *N*-(methyl-d_3)-aniline in the presence of **1b-Nb** (Scheme 9). Consistent with our previous findings, high retention of deuterium in the methylene position and high deuteration of the cyclic methylene group were observed. The delivery of deuterium to the ring proceeded exclusively to the *exo*-position, thus yielding the *syn*-insertion isomer of **8** (isolated as benzylamide **12-D**). These results are in agreement with observations of Milstein et al. on iridium-catalyzed hydroamination of norbornene with aniline.[21] Most interestingly, the deuterated benzylamide **12-D** was formed with significant lower enantioselectivity (30% ee) in comparison to the undeuterated congener **12** (59% ee).

While the *syn*-addition to the olefin is consistent with the inner-sphere olefin insertion mechanism and, therefore, is an

Scheme 9

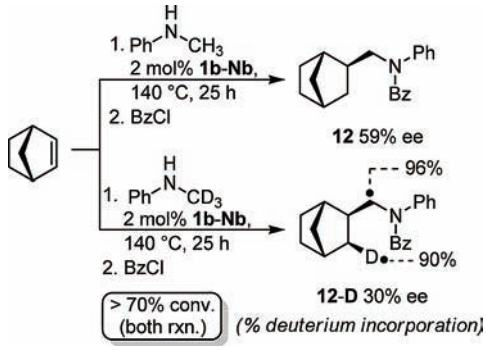

expected result, the significant perturbation of enantioselectivity in the formation of **12-D** caused by the isotopic substitution is striking. As the stereodetermining step itself (insertion, step 2) does not directly involve the cleavage or formation of a C−H bond as the protonolysis (step 3) does, the perturbation of enantioselectivity suggests that step 2 is reversible[21,22] and is faster than intramolecular protonolysis (Scheme 10, a). The

Scheme 10. Scenarios for Isotopic Perturbation of Enantioselectivity in the Hydroaminoalkylation of Norbornene: (a) Reversible Olefin Insertion and Slow Intramolecular Protonolysis. (b) Concerted Insertion-Protonolysis

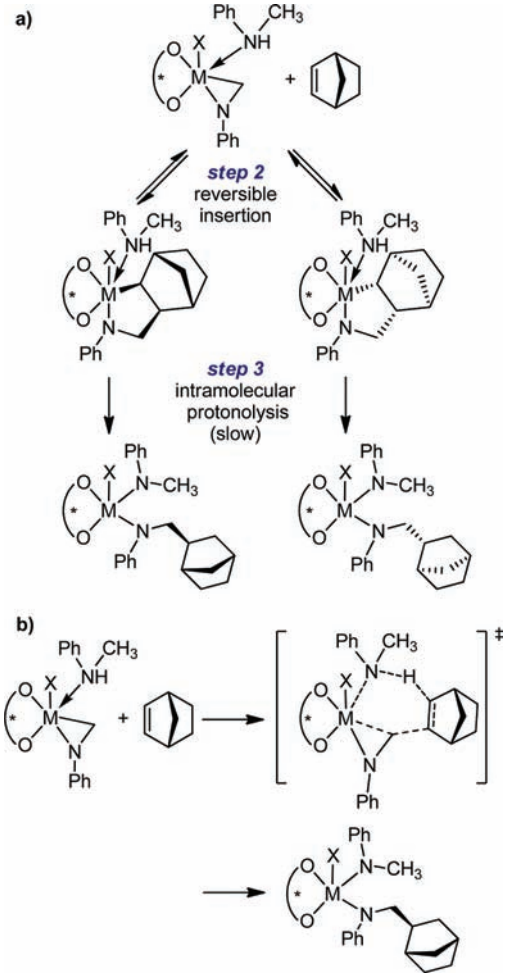

dx.doi.org/10.1021/ja211945m | J. Am. Chem. Soc. 2012, 134, 3300−3311

fact that this phenomenon is observed in the case of norbornene is likely due to the fact that the intramolecular protonolysis (step 3) involves proton transfer to a more sterically hindered methine carbon as opposed to the methylene group in the case of α-olefins. Indeed, no perturbation of enantioselectivity was observed in the case of α-olefins: 73% ee versus 73% ee for **4a-D** and **4a** and 79.5% ee versus 80% ee for **6a-D** and **6a**, respectively, thus strongly suggesting an effectively irreversible insertion (step 2) and fast intramolecular protonolysis (step 3).

An alternative explanation for the observed perturbation of enantioselectivity would involve a concerted insertion-protonolysis step with participation of a coordinated amine, which is both stereodetermining and involves the conversion of an N–H bond into a C–H bond (Scheme 10, b). This scenario was used to explain the isotopic perturbation of enantioselectivity in the zirconium-catalyzed intramolecular hydroamination of aminoalkenes.[16d,h] However, this proposal does not explain the unique behavior of norbornene with respect to the perturbation of enantioselectivity as found in this study. Furthermore, the concerted insertion-protonolysis sequence recently proposed for a magnesium hydroamination catalyst system[16c] was found to proceed via fast reversible insertion and rate-determining protonolysis according to DFT calculations.[23]

Empirical Rate Laws. To determine the empirical rate laws, a kinetic investigation of the hydroaminoalkylation of *N*-methyl-anilines **2a–d** with 1-octene and vinylcyclohexane using **1b-Nb** was performed. The reaction displays a relatively well-behaved first-order kinetic behavior in **2** over the course of 2–3 half-lives in the presence of an excess of alkene. The observed first-order rate constant is linearly dependent on the catalyst concentration **1b-Nb** (Figure 1), therefore, indicating a first-order dependence in **2** and **1b-Nb**.

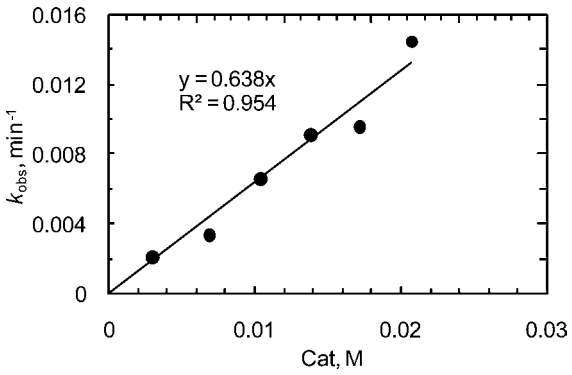

Figure 1. Dependence of observed first-order reaction constant on catalyst concentration for the reaction of 1-octene (0.613 M) with PMPNHMe (**2d**) (0.20 M) in the presence of (*R*)-**1b-Nb** (0.003–0.022M) in C_6D_6 at 150 °C. The line represents the least-squares fit to the data points.

Although a first-order rate dependence on catalyst concentration is in a good agreement with a well-defined monometallic species participating in the catalytic reaction, it should be noted that a nonlinear saturation behavior was recently reported for the intramolecular aminoalkene hydroaminoalkylation catalyzed by **IVb**.[6f]

An attempt to determine the reaction order in alkene showed a pronounced discrepancy between nonhindered (1-octene) and hindered (vinylcyclohexane) alkenes (Figure 2).

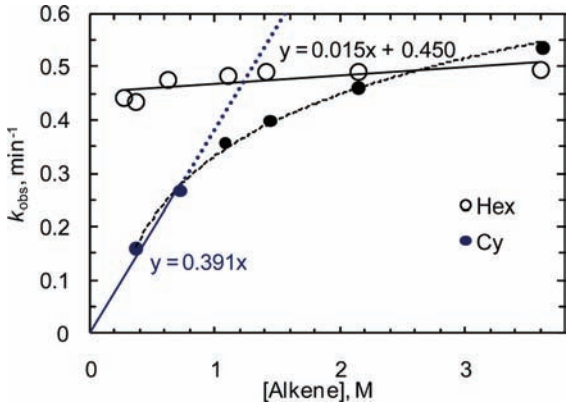

Figure 2. Dependence of pseudo-first-order rate constant on alkene concentration for the reaction of 1-octene (0.26–3.75 M) (○) and vinylcyclohexane (0.29–3.75 M) (●) with PMPNHMe (**2d**) (0.29 M) in the presence of (*R*)-**1b-Nb** (0.017 M) in C_6D_6 at 150 °C. The solid lines represent the least-squares fit to the data points; dotted lines are drawn as a guide for the eye.

Essentially no rate dependence on the concentration of 1-octene was observed, which indicates that alkene insertion (Scheme 6, step 2) is not rate-determining and is proceeding relatively fast within a large concentration interval of the alkene. Saturation behavior was observed in case of the sterically more demanding vinylcyclohexane with the rate being close to zero-order in alkene at high alkene concentrations, while first-order dependence was apparent at low alkene concentrations. Thus, insertion step 2 can serve as a rate-determining step as well. On the basis of these results, an empirical rate law can be proposed (eq 1).

$$\text{rate} = k[\textbf{1b-Nb}][\textbf{2}][\text{alkene}]^{\alpha} \quad \text{with } 0 \le \alpha \le 1 \qquad (1)$$

The insertion step (Scheme 6, step 2) is sensitive to the steric features of the alkene and **2a–d** react with vinylcyclohexane and 1-octene with comparable rates in the saturation regime. The first-order rate dependence on the concentration of *N*-methyl-anilines **2a–d** (Figure 3, see also

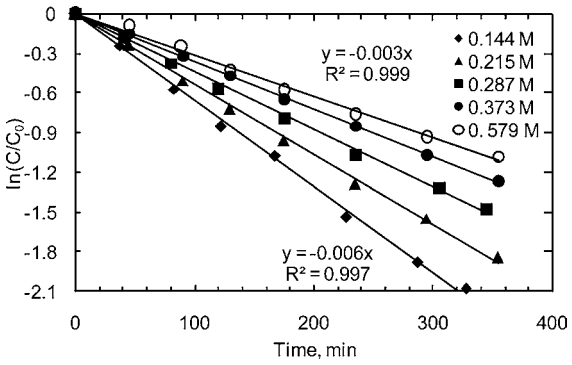

Figure 3. First-order kinetic plots for the reaction of 1-octene (0.613 M) with 4-FC_6H_4NHMe (**2b**) (0.144–0.579 M) in the presence of (*R*)-**1b-Nb** (0.017 M) in C_6D_6 at 150 °C. The solid lines represent the least-squares fit to the data points.

Supporting Information) is indicative of amide exchange (Scheme 6, step 4) becoming rate-determining at high alkene concentrations.

In the presence of an excess of 1-octene (zero-order in alkene), the reaction can be adequately described as being first-

dx.doi.org/10.1021/ja211945m | *J. Am. Chem. Soc.* 2012, 134, 3300–3311

order in **2** at all alkene concentrations. However, reactions at high amine concentrations are significantly slower, which indicates a pronounced amine inhibition. This inhibition may originate from reversible metallaaziridine formation (step 1) or from other nonproductive events which may involve **1b-Nb** and **2**. As clearly demonstrated above, although step 1 is reversible, the nondissociative character of this transformation implies that neither the elimination step (Scheme 6, step 1) nor its reversal should depend on the concentration of free **2**, and therefore, this inhibition scenario can be ruled out. Instead, it seems more likely that the inhibition pathway involves reversible nonproductive binding of the free amine (either **2** or **4**) to the catalytically active five-coordinate bis(anilide) **A** to form a "dormant" six-coordinate species **AL** (Scheme 11).

Scheme 11. Equilibrium between Catalytic Active Five-Coordinate Species A and Its "Dormant" Amine Adduct

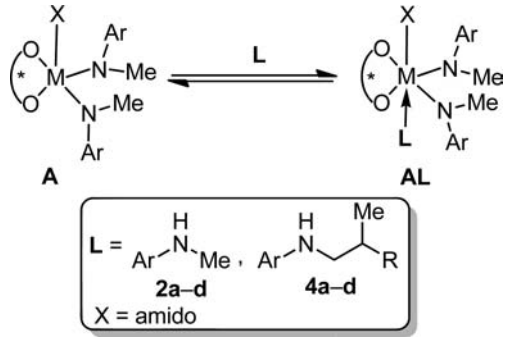

The ability of the niobium center to adopt a six-coordinate environment is justified by the formation of the amine-coordinated aziridine (**A*PhNHMe**) elucidated by isotopic labeling. Furthermore, many of the precatalysts **1a–d** include an additional coordinated amine molecule.[8,12] The inhibition operating via nonproductive binding of an additional substrate equivalent is also rather common in early transition metal-catalyzed hydroamination.[16a,d,e,24,25]

Kinetic Isotope Effects. Determination of the kinetic isotope effect (KIE) has proven to be a very useful mechanistic tool, which has been applied in many studies of C–H activation by organometallic systems.[26] We performed the reaction of **2a**, **2a-ND**, and **2a-CD$_3$** with 1-octene in the presence of **1b-Nb**; however, in the absence of a complete mechanistic and kinetic model, the observed kinetic isotope effects for nonelementary transformations should be interpreted very carefully.

As shown in Figure 4, N-deuteration of **2a** resulted in a primary KIE of 1.6 ± 0.1, whereas deuteration of the methyl group in **2a-CD$_3$** did not significantly diminish the rate of the reaction. This result suggests that the C–H activation (step 1) is unlikely to be rate-determining under these conditions, whereas the rate-determining amide exchange (step 4) can account for the primary KIE as the N–H bond is being formed and broken during this step. These findings are in remarkable contrast to the strong primary isotope effect observed in intramolecular hydroaminoalkylation of a C-deuterated aminoalkene by Doye.[6f] More detailed studies of the KIEs will be described below as we will proceed by introducing a mechanistic model that will account for all mechanistic and kinetic observations.

Mechanistic Model for Asymmetric Hydroaminoalkylation. The proposed mechanistic model is depicted in Scheme

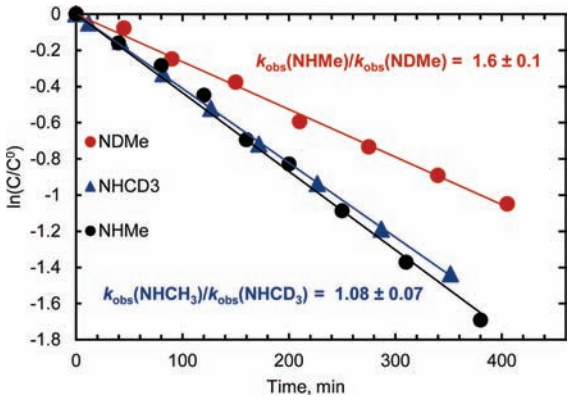

Figure 4. First-order kinetic plots for the reaction of 1-octene (1.89 M) with PhNHMe (**2a**) and its deuterated analogues (0.311 M) in the presence of (*R*)-**1b-Nb** (0.019 M) in C_6D_6 at 150 °C. The solid lines represent the least-squares fit to the data points.

12. Protonolysis of precatalyst **1-Nb** with an excess of substrate **S** liberates two molecules of dimethylamine and yields the

Scheme 12. Proposed Mechanism for the Intermolecular Hydroaminoalkylation

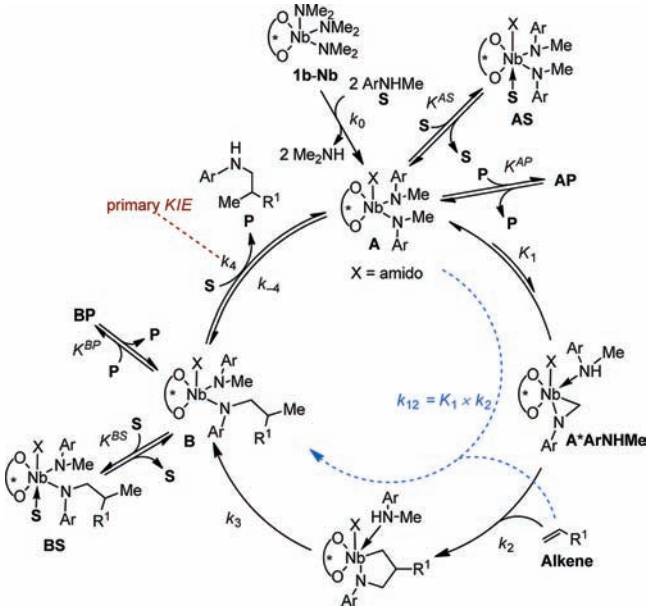

bisamide **A**, which subsequently undergoes intramolecular rearrangement to the six-coordinate metallaaziridine **A*ArNHMe**. The metallaaziridine undergoes intermolecular alkene insertion, followed by intramolecular protonolysis to yield the bisamide **B**, which may regenerate the bisamide **A** and release the product **P** via reversible amide exchange with an additional substrate molecule **S**. Reversible nonproductive binding of **S** and **P** to bisamides **A** and **B** yields six-coordinate bisamides **AS**, **AP**, **BS**, and **BP**.

Based on the assumptions that

1. catalyst activation is fast compared to catalytic turnover;
2. $K_1 < 0.05$ and the concentration of the metallaaziridine **A*ArNHMe** is small at all times;
3. the transformation from **A** to **B** can be described by a combined rate constant $k_{12} = K_1k_2$;

dx.doi.org/10.1021/ja211945m | *J. Am. Chem. Soc.* 2012, 134, 3300–3311

4. all inhibition equilibrium constants have similar values ($K^{AS} \approx K^{AP} \approx K^{BS} \approx K^{BP} \equiv K^{dorm}$);
5. the bimolecular amide exchange constants are very similar in value ($k_4 \approx k_{-4}$);
6. catalyst loadings are low ($[cat]_0 \ll [S]_0$);

one can derive eq 2 using a steady state approach (see Supporting Information for details).

$$\text{rate} = \frac{k_{12}k_4[\text{cat}]_0[\text{S}][\text{alkene}]}{k_4[\text{S}]_0 + k_{12}[\text{alkene}]} \frac{1}{1 + K^{\text{dorm}}[\text{S}]_0} \quad (2)$$

Equation 2 can be simplified for two limiting cases. (1) Alkene insertion is faster than amide exchange ($k_{12}[\text{alkene}] \gg k_4[\text{S}]_0$):

$$\text{rate} = k_{\text{obs}}[\text{cat}]_0[\text{S}] \quad (3)$$

$$\text{with } k_{\text{obs}} = \frac{k_4}{1 + K^{\text{dorm}}[\text{S}]_0}$$

In this case, the reaction will be limited by amide exchange and will display zero-order rate dependence on alkene concentration as observed for the fast insertion of 1-octene and high concentrations of vinylcyclohexane.

(2) If alkene insertion is rate-limiting ($k_{12}[\text{alkene}] \ll k_4[\text{S}]_0$), one should observe an overall third-order reaction (eq 4).

$$\text{rate} = k_{\text{obs}}[\text{cat}]_0[\text{S}][\text{alkene}] \quad (4)$$

$$\text{with } k_{\text{obs}} = \frac{k_{12}}{[\text{S}]_0\left(1 + K^{\text{dorm}}[\text{S}]_0\right)}$$

Certain assumptions introduced in the derivation of eq 2, such as low catalyst loadings, restrict its broader applicability. A numerical nonlinear regression approach allows handling of complicated kinetic models without the aforementioned restrictions. Thus, analysis of kinetic data for the reaction of **2b** with 1-octene employing models of different complexity using the program DynaFit[27] allows evaluation of our assumptions on the relative turnover and equilibrium constant values (see Supporting Information for details). The most primitive model (assumption: $k_4 = k_{-4}$ and $K^{AS} = K^{AP} = K^{BS} = K^{BP} = K^{dorm}$) showed a good fit to the experimental data (Figure 5). Thus, the assumptions on the values for the different inhibition and amide exchange rate constants used in the derivation of eq 3 were indeed justified.

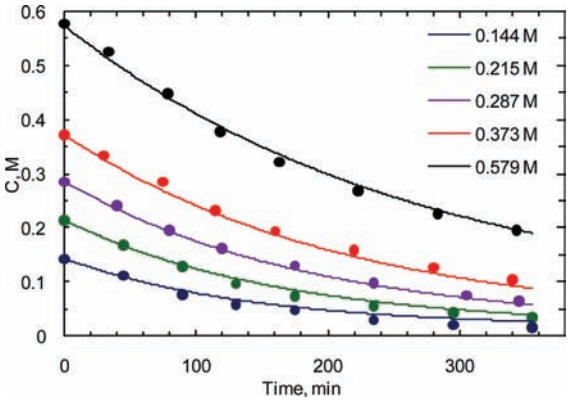

Figure 5. Experimental reaction progress data (dots) for the reaction of 1-octene (0.613 M) with **2b** (0.144–0.579 M) in the presence of (*R*)-**1b-Nb** (0.017 M) in C_6D_6 at 150 °C vs the simulated reaction curves (lines) for $k_4 = 0.58 \pm 0.09$ M^{-1} min^{-1}, $K^{dorm} = 2.8 \pm 0.7$ M^{-1}.

This kinetic model was also applied to the nonlinear regression analysis of the kinetic data of the reactions of 1-octene with other *N*-methyl-aniline derivatives (Table 3).

Deuteration of the N-methyl group in **2a-CD$_3$** did not result in a measurable KIE for k_4 or an equilibrium isotope effect (EIE) for K^{dorm}. Because k_4 describes the amide exchange reaction in which no C–H bond is formed or broken, the absence of a KIE matches the mechanistic expectations. In contrast, the *N*-deutero substrate **2a-ND** displayed a primary KIE of 1.8 ± 0.3, which is in agreement with the value obtained from observed constants (Figure 4). The accuracy of the measurements is insufficient to decide whether an EIE for the reversible nonproductive amine binding is present or not.

The dependence of kinetic parameters on the electronic properties of the *para*-substituent is nonlinear for both k_4 and K^{dorm}. *N*-Methyl-aniline (**2a**) is less prone to inhibition and is reacting slower than the more electron-accepting halide-substituted **2b** and **2c**, whereas the electron-donating methoxy-substituted **2d** is most reactive (Figure 6).

It can be speculated that the observed nonlinearity may in part originate from the complex character of the interaction of **2** with **A** or **B** (Scheme 12), whether as an amide or amine. Indeed, the more nucleophilic and more Lewis-basic substrate **2d** should form stronger covalent and dative bonds to the metal than **2a**. While **2c** itself is more electron-deficient and should be less reactive, the corresponding species **A** contains two electron-deficient anilide ligands and is, therefore, more electrophilic and prone to amine inhibition. The overall reactivity is controlled by the interplay of the electronic features of ligand and starting material. Thus, it is expected that catalysts with a more electron-deficient ligand backbone should possess enhanced reactivity.

To get further insight into the kinetics of the process and obtain the values of the insertion constant k_{12}, we performed a detailed kinetic study for the reaction of **2** with vinylcyclohexane at various alkene concentrations. The kinetic data was subjected to a nonlinear least-squares fit according to the mechanism in Scheme 12. As demonstrated above, substrate and product inhibition is comparable to that for the reactions with 1-octene. Therefore, the values of K^{dorm} obtained for 1-octene may be used in the nonlinear fit for vinylcyclohexane (Table 4). Again, the results from the numerical fitting were in good agreement with experimental data (Figure 7).

A majority of amide exchange rate constants k_4 obtained for the reaction of **2a–d** with vinylcylohexane (Table 4) are in good agreement to those obtained for the reaction with 1-octene (Table 3). The observed insertion constants k_{12} display nonlinear dependence on the electronic properties of the substrate. However, since k_{12} is a nonelementary rate constant derived from the equilibrium constant K_1 and the "true" insertion constant k_2, the absolute value of k_{12} should be interpreted carefully. Notably, a similar nonlinear correlation was observed for the zirconaaziridine formation from a (methyl)anilidozirconium species via methane elimination.[28]

An important observation is the negligible KIE for **3d**: $k_{12}(CH_3)/k_{12}(CD_3) = 1.19 \pm 0.14$. This suggests that no strong primary KIE or EIE is associated with the aziridine formation, as olefin insertion should not display any primary KIE. Alternatively, if the insertion proceeds in a concerted fashion with intramolecular protonolysis, this reaction can exhibit a

dx.doi.org/10.1021/ja211945m | *J. Am. Chem. Soc.* 2012, 134, 3300–3311

Table 3. Kinetic Parameters for the Reaction of 2a-d with 1-Octene[a]

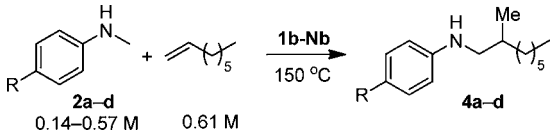

entry	R	k_4, M^{-1} min^{-1}	K^{dorm}, M^{-1}
1	H (**2a**)	0.33 ± 0.02	1.6 ± 0.3
2	H (**2a-CD$_3$**)	0.38 ± 0.05	1.9 ± 0.5
3	H (**2a-ND**)	0.18 ± 0.03	1.1 ± 0.6
4	F (**2b**)	0.58 ± 0.09	2.8 ± 0.7
5	Cl (**2c**)	0.58 ± 0.15	7.8 ± 2.4
6	MeO (**2d**)	3.1 ± 1.2	14.4 ± 5.0

[a]Nonlinear fit to a fast insertion model ($k_{12} \gg k_4 = k_{-4}$ and $K^{AS} = K^{AP} = K^{BS} = K^{BP} = K^{dorm}$), confidence intervals for 95% probability.

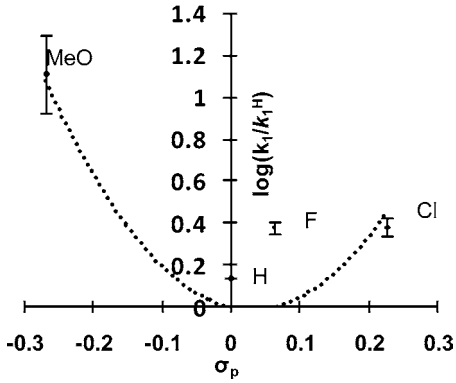

Figure 6. Hammett plot for turnover constant k_4 for the reaction of **2a–d** with 1-octene. Error bars indicate the error of the measurement. The dotted line is drawn as a guide for the eye.

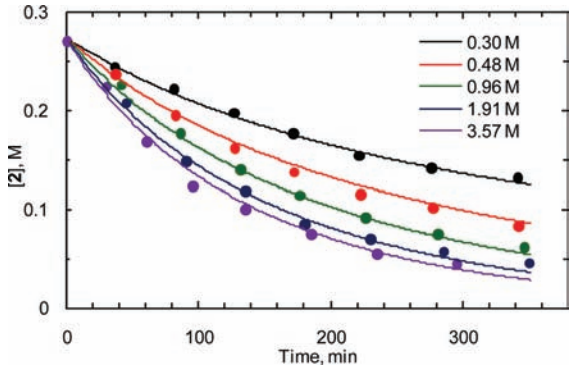

Figure 7. Experimental reaction progress data (dots) for the reaction of vinylcylohexane (0.30–3.57 M) with PMPNHCH$_3$ (**2d**) (0.270 M) in the presence of (*R*)-**1b-Nb** (0.017 M) in C_6D_6 at 150 °C versus the simulated reaction curves (lines) for k_4 = (3.7 ± 0.2) M^{-1} min^{-1}, k_{12} = (0.81 ± 0.05) M^{-1} min^{-1}, K^{dorm} = 14.4 M^{-1}. The value of K^{dorm} was obtained from the reaction with 1-octene.

primary KIE, because the hydrogen (respectively, deuterium) in the N–H bond (respectively, N–D bond) that is being broken originates from the methyl group of the *N*-methylaniline. The negligible net KIE can originate from the superposition of the primary KIE for insertion-protonolysis and the inverse EIE for the aziridine formation. At this point none of these scenarios can be ruled out with certainty. It should be noted that the absence of isotopic perturbation of enantioselectivity for the reaction involving 1-octene and vinylcyclohexane is a strong argument against a concerted insertion-protonolysis mechanism. The stereodetermining step would involve cleavage of the N–H bond and one would expect some variation of stereoselectivity, which has been frequently observed in hydroamination reactions.[16a,d,h]

Although norbornene displayed a remarkable isotopic perturbation of enantioselectivity, it is prone to polymerization under the standard reaction conditions and reliable kinetic data could not be obtained. Overall, the absence of a primary KIE in the isolated reaction step directly involving the formation of the metallaaziridine is in remarkable contrast to literature precedence of metallaaziridine formation in titanium-catalyzed hydroaminoalkylations,[6f] as well as in stoichiometric metallaaziridine formation via elimination of an alkane.[28,29]

Table 4. Kinetic Parameters for the Reaction of 2a–d with Vinylcyclohexane[a]

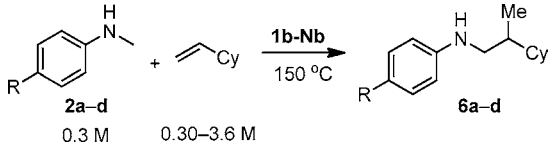

entry	R	k_4, M^{-1} min^{-1}	k_{12}, M^{-1} min^{-1}[b]
1	H (**2a**)	0.39 ± 0.03	0.31 ± 0.05
2	F (**2b**)	0.89 ± 0.05	0.35 ± 0.02
3	Cl (**2c**)	0.67 ± 0.03	0.56 ± 0.07
4	MeO (**2d**)	3.7 ± 0.2	0.81 ± 0.05
5	MeO (**2d-CD$_3$**)	3.0 ± 0.3	0.68 ± 0.07

[a]Nonlinear fit to a slow insertion model ($k_{12} \neq k_4 = k_{-4}$ and $K^{AS} = K^{AP} = K^{BS} = K^{BP} = K^{dorm}$), confidence intervals for 95% probability. [b]Value for major enantiomer.

dx.doi.org/10.1021/ja211945m | *J. Am. Chem. Soc.* 2012, 134, 3300–3311

CONCLUSIONS

Group 5 metal binaphtholate complexes are highly active catalysts in the intermolecular hydroaminoalkylation of unactivated alkenes with secondary amines. The reaction proceeds with high enantio- and regioselectivity (up to 98% ee, branched products formed exclusively). The strong preference to activate primary amine α-C−H bonds originate from steric constrains hampering alkene insertion, as demonstrated by isotopic labeling experiments. Mechanistic studies suggest that the reaction proceeds via a reversible, nondissociative formation of a six-coordinate metallaaziridine species, which undergoes facile alkene insertion and subsequent intramolecular protonolysis. Kinetic studies are supportive of a monometallic catalytic pathway with either alkene insertion or amide exchange serving as a rate-determining step. The amide exchange step is marked by a primary KIE, whereas essentially no KIE was observed for the aziridine formation/olefin insertion/protonolysis sequence. The latter result is in remarkable contrast to previous findings in metallaaziridine chemistry and should originate from stereoelectronic effects of the binaphtholate ligand. Simulation experiments show a good fit of the proposed kinetic model to the original kinetic data. Reversible nonproductive events include amine coordination to the catalytically active species and C−H activation of the aromatic ring for the tantalum catalysts. All turnover and equilibrium constants displayed nonlinear dependence on the electronic properties of the amine substrate. Evidence of an electron-acceptor ligand favoring the amide exchange process was obtained, which can be used as a guideline for future catalyst developments. These studies along with work toward the development of sterically more accessible catalysts for hydroaminoalkylation of secondary C−H bonds will be further pursued by our laboratory.

ASSOCIATED CONTENT

Supporting Information

Experimental procedures and characterization data, NMR spectra of all new ligands, complexes and products, HPLC traces, details of kinetic experiments and simulations. This material is available free of charge via the Internet at http://pubs.acs.org.

AUTHOR INFORMATION

Corresponding Author

hultzsch@rci.rutgers.edu

Notes

The authors declare no competing financial interest.

ACKNOWLEDGMENTS

This work was supported by the National Science Foundation through a NSF CAREER Award (CHE 0956021).

REFERENCES

(1) (a) Roesky, P. W. *Angew. Chem., Int. Ed.* **2009**, *48*, 4892. (b) Eisenberger, P.; Schafer, L. L. *Pure Appl. Chem.* **2010**, *82*, 1503.

(2) The hydroaminoalkylation, as discussed in this article, should be distinguished from the hydroaminomethylation reaction that proceeds via a tandem hydroformylation/reductive amination sequence, see: (a) Eilbracht, P.; Bärfacker, L.; Buss, C.; Hollmann, C.; Kitsos-Rzychon, B. E.; Kranemann, C. L.; Rische, T.; Roggenbuck, R.; Schmidt, A. *Chem. Rev.* **1999**, *99*, 3329. (b) Beller, M.; Seayad, J.; Tillack, A.; Jiao, H. *Angew. Chem., Int. Ed.* **2004**, *43*, 3368.

(3) For other functionalizations of sp^3-hybridized α-amino C−H moieties see: (a) Campos, K. R. *Chem. Soc. Rev.* **2007**, *36*, 1069. (b) Li, C.-J. *Acc. Chem. Res.* **2009**, *42*, 335. (c) DeBoef, B.; Pastine, S. J.; Sames, D. *J. Am. Chem. Soc.* **2004**, *126*, 6556. (d) Yi, C. S.; Yun, S. Y.; Guzei, I. A. *Organometallics* **2004**, *23*, 5392. (e) Wan, X.; Xing, D.; Fang, Z.; Li, B.; Zhao, F.; Zhang, K.; Yang, L.; Shi, Z. *J. Am. Chem. Soc.* **2006**, *128*, 12046. (f) Pastine, S. J.; Gribkov, D. V.; Sames, D. *J. Am. Chem. Soc.* **2006**, *128*, 14220. (g) Murahashi, S.-I.; Nakae, T.; Terai, H.; Komiya, N. *J. Am. Chem. Soc.* **2008**, *130*, 11005.

(4) (a) Clerici, M. G.; Maspero, F. *Synthesis* **1980**, 305. (b) Nugent, W. A.; Ovenall, D. W.; Holmes, S. J. *Organometallics* **1983**, *2*, 161.

(5) For hydroaminoalkylations catalyzed by group 5 metal complexes see: (a) Herzon, S. B.; Hartwig, J. F. *J. Am. Chem. Soc.* **2007**, *129*, 6690. (b) Herzon, S. B.; Hartwig, J. F. *J. Am. Chem. Soc.* **2008**, *130*, 14940. (c) Eisenberger, P.; Ayinla, R. O.; Lauzon, J. M. P.; Schafer, L. L. *Angew. Chem., Int. Ed.* **2009**, *48*, 8361. (d) Zi, G.; Zhang, F.; Song, H. *Chem. Commun.* **2010**, *46*, 6296. (e) Zhang, F.; Song, H.; Zi, G. *Dalton Trans.* **2011**, *40*, 1547.

(6) For hydroaminoalkylations catalyzed by group 4 metal complexes see: (a) Müller, C.; Saak, W.; Doye, S. *Eur. J. Org. Chem.* **2008**, 2731. (b) Kubiak, R.; Prochnow, I.; Doye, S. *Angew. Chem., Int. Ed.* **2009**, *48*, 1153. (c) Prochnow, I.; Kubiak, R.; Frey, O. N.; Beckhaus, R.; Doye, S. *ChemCatChem* **2009**, *1*, 162. (d) Bexrud, J. A.; Eisenberger, P.; Leitch, D. C.; Payne, P. R.; Schafer, L. L. *J. Am. Chem. Soc.* **2009**, *131*, 2116. (e) Kubiak, R.; Prochnow, I.; Doye, S. *Angew. Chem., Int. Ed.* **2010**, *49*, 2626. (f) Prochnow, I.; Zark, P.; Müller, T.; Doye, S. *Angew. Chem., Int. Ed.* **2011**, *50*, 6401.

(7) For hydroaminoalkylations catalyzed by late transition metals see: (a) Jun, C.-H.; Hwang, D.-C.; Na, S.-J. *Chem. Commun.* **1998**, 1405. (b) Chatani, N.; Asaumi, T.; Yorimitsu, S.; Ikeda, T.; Kakiuchi, F.; Murai, S. *J. Am. Chem. Soc.* **2001**, *123*, 10935. (c) Pan, S.; Endo, K.; Shibata, T. *Org. Lett.* **2011**, *13*, 4692.

(8) Reznichenko, A. L.; Emge, T. J.; Audörsch, S.; Klauber, E. G.; Hultzsch, K. C.; Schmidt, B. *Organometallics* **2011**, *30*, 921.

(9) Horrillo-Martínez, P.; Hultzsch, K. C.; Gil, A.; Branchadell, V. *Eur. J. Org. Chem.* **2007**, 3311.

(10) (a) Wood, M. C.; Leitch, D. C.; Yeung, C. S.; Kozak, J. A.; Schafer, L. L. *Angew. Chem., Int. Ed.* **2007**, *46*, 354. (b) Gott, A. L.; Clarke, A. J.; Clarkson, G. J.; Scott, P. *Organometallics* **2007**, *26*, 1729. (c) Reznichenko, A. L.; Hultzsch, K. C. *Organometallics* **2010**, *29*, 24. (d) Zi, G.; Zhang, F.; Xiang, L.; Chen, Y.; Fang, W.; Song, H. *Dalton Trans.* **2010**, *39*, 4048. (e) Ayinla, R. O.; Gibson, T.; Schafer, L. L. *J. Organomet. Chem.* **2011**, *696*, 50.

(11) Cummings, S.; Tunge, J. A.; Norton, J. R. *Top. Organomet. Chem.* **2005**, *10*, 1.

(12) Rothwell has synthesized and structurally characterized some of the binaphtholate tantalum complexes discussed in this study; however, no catalytic results have been reported, see: (a) Thorn, M. G.; Moses, J. E.; Fanwick, P. E.; Rothwell, I. P. *J. Chem. Soc., Dalton Trans.* **2000**, 2659. (b) Ru Son, A. J.; Schweiger, S. W.; Thorn, M. G.; Moses, J. E.; Fanwick, P. E.; Rothwell, I. P. *Dalton Trans.* **2003**, 1620.

(13) Reznichenko, A. L.; Nguyen, H. N.; Hultzsch, K. C. *Angew. Chem., Int. Ed.* **2010**, *49*, 8984.

(14) Hoffmann, S.; Nicoletti, M.; List, B. *J. Am. Chem. Soc.* **2006**, *128*, 13074.

(15) (a) Watson, P. L.; Parshall, G. W. *Acc. Chem. Res.* **1985**, *18*, 51. (b) Thompson, M. E.; Baxter, S. M.; Bulls, A. R.; Burger, B. J.; Nolan, M. C.; Santarsiero, B. D.; Schaefer, W. P.; Bercaw, J. E. *J. Am. Chem. Soc.* **1987**, *109*, 203. (c) Fendrick, C. M.; Marks, T. J. *J. Am. Chem. Soc.* **1986**, *108*, 425. (d) Sadow, A. D.; Tilley, T. D. *J. Am. Chem. Soc.* **2003**, *125*, 7971.

(16) (a) Gagné, M. R.; Stern, C. L.; Marks, T. J. *J. Am. Chem. Soc.* **1992**, *114*, 275. (b) Allan, L. E. N.; Clarkson, G. J.; Fox, D. J.; Gott, A. L.; Scott, P. *J. Am. Chem. Soc.* **2010**, *132*, 15308. (c) Dunne, J. F.; Fulton, D. B.; Ellern, A.; Sadow, A. D. *J. Am. Chem. Soc.* **2010**, *132*, 17680. (d) Manna, K.; Xu, S.; Sadow, A. D. *Angew. Chem., Int. Ed.* **2011**, *50*, 1865. (e) Arrowsmith, M.; Crimmin, M. R.; Barrett, A. G. M.; Hill, M. S.; Kociok-Köhn, G.; Procopiou, P. A. *Organometallics* **2011**, *30*, 1493. (f) Leitch, D. C.; Platel, R. H.; Schafer, L. L. *J. Am.*

Chem. Soc. **2011**, *133*, 15453. (g) Hangaly, N. K.; Petrov, A. R.; Rufanov, K. A.; Harms, K.; Elfferding, M.; Sundermeyer, J. *Organometallics* **2011**, *30*, 4544. (h) Manna, K.; Kruse, M. L.; Sadow, A. D. *ACS Catal.* **2011**, *1*, 1637. (i) Zhang, X.; Emge, T. J.; Hultzsch, K. C. *Angew. Chem., Int. Ed.* **2012**, *51*, 394.
(17) (a) Hanley, P. S.; Markovic, D.; Hartwig, J. F. *J. Am. Chem. Soc.* **2010**, *132*, 6302. (b) Hanley, P. S.; Hartwig, J. F. *J. Am. Chem. Soc.* **2011**, *133*, 15661.
(18) (a) Neukom, J. D.; Perch, N. S.; Wolfe, J. P. *J. Am. Chem. Soc.* **2010**, *132*, 6276. (b) Neukom, J. D.; Perch, N. S.; Wolfe, J. P. *Organometallics* **2011**, *30*, 1269. (c) White, P. B.; Stahl, S. S. *J. Am. Chem. Soc.* **2011**, *133*, 18594.
(19) Zhang, J.; Yang, C.-G.; He, C. *J. Am. Chem. Soc.* **2006**, *128*, 1798.
(20) McKinney Brooner, R. E.; Widenhoefer, R. A. *Chem.—Eur. J.* **2011**, *17*, 6170.
(21) Casalnuovo, A. L.; Calabrese, J. C.; Milstein, D. *J. Am. Chem. Soc.* **1988**, *110*, 6738.
(22) (a) Gallazzi, M. C.; Porri, L.; Vitulli, G. *J. Organomet. Chem.* **1975**, *97*, 131. (b) Catellani, M.; Motti, E.; Della Cá, N. *Acc. Chem. Res.* **2008**, *41*, 1512. (c) Martins, A.; Mariampillai, B.; Lautens, M. *Top. Curr. Chem.* **2010**, *292*, 1.
(23) Tobisch, S. *Chem.—Eur. J.* **2011**, *17*, 14974.
(24) Gribkov, D. V.; Hultzsch, K. C.; Hampel, F. *J. Am. Chem. Soc.* **2006**, *128*, 3748.
(25) Hong, S.; Kawaoka, A. M.; Marks, T. J. *J. Am. Chem. Soc.* **2003**, *125*, 15878.
(26) (a) Parkin, G. *Acc. Chem. Res.* **2009**, *42*, 315. (b) Gómez-Gallego, M.; Sierra, M. A. *Chem. Rev.* **2011**, *111*, 4857.
(27) Kuzmič, P. *Anal. Biochem.* **1996**, *237*, 260.
(28) Coles, N.; Harris, M. C. J.; Whitby, R. J.; Blagg, J. *Organometallics* **1994**, *13*, 190.
(29) Mayer, J. M.; Curtis, C. J.; Bercaw, J. E. *J. Am. Chem. Soc.* **1983**, *105*, 2651.